Earthquakes and Structures, *Vol. 21, No. 1 (2021) 17-27*
DOI: https://doi.org/10.12989/eas.2021.21.7.017

Post-earthquake fire resistance of tall steel concentrically braced frames

Rasul Kaffash[a] and Abbas Karamodin[*]

Department of Civil Engineering, Ferdowsi University of Mashhad, Iran

(Received April 8, 2020, Revised May 11, 2021, Accepted June 7, 2021)

Abstract. The fire which occurs after an earthquake causes great problems for buildings situated in moderate to high seismic regions. In this article in order to have an understanding regarding the impacts of post-earthquake fire on the structures, implementing the finite element method, the behaviour of tall steel concentrically braced frames when subjected to this type of loading was investigated. The simulation under seismic loading was done using the nonlinear time history analysis. Assuming the post-earthquake situation of the structure as the initial condition, the mechanical-thermal analysis was applied using the temperature-time diagram on the exposed elements. The analysis results showed that regardless of the earthquake record and fire scenarios for the tall steel concentrically braced frames, the fire resistance duration was short and the impacts of the previous earthquake on the structure fire resistance were not considerable.

Keywords: fire following earthquake; multi-stage analysis; fire resistance; concentrically braced frames; overall behaviour

1. Introduction

Reviewing the past real fire events after earthquake shows that it may cause considerable damage in buildings (Scawthorn, Eidinger *et al*. 2005). However, the post-earthquake fire with the potential of causing extensive damage in structures has not been yet considered as a loading case in the present design codes (Behnam 2016). In addition, the current seismic design regulations allow a certain amount of damage in structure after experiencing an earthquake, this issue could increase the system vulnerability to fire. Up to now limited research have been performed on the global response of the steel structures when subjected to a post-earthquake fire.

One of the first studies was conducted by Della Corte *et al* (2005). They have developed a number of numerical models to assess the performance of steel moment resisting frames under the fire which follows after an earthquake. It was understood that the philosophy behind the seismic design of a structure could greatly influence the performance of steel moment resisting frames subjected to post-earthquake fire.

Performance based fire resistant of structures has been studied by many researchers. Faggiano *et al*. (2007) assessed the performance of steel portal frames when subjected to post-earthquake fire and found that the collapse mechanism and fire resistance of portal frames under post-earthquake fire were similar to the case where the frames did not exceed the operational performance limit during the earthquake. Therefore, a negligible reduction was observed in the life safety and collapse levels. The performance of steel structures under the post-earthquake fire scenarios was presented by Faggiano *et al*. (2010) which were comprised of the Operational Fire, immediate Occupancy Fire, Life Safety Fire, and Collapse Prevention Fire ones. In their investigation the seismic damages to the structures and also their resistance to fire following the earthquake were examined.

Zaharia and Pintea (2009) have studied the effect of earthquake intensity on response of structures under post-earthquake fire. They examined two steel frames with two earthquakes return periods of 2475 and 475 years using the pushover analysis. The results of their earthquake analysis showed that the frame designed for 2475 years return period remained in elastic state, whereas the frame with 475 years return period (weaker frame) experienced considerable story drift. Also, consequent fire analysis performed for both frames showed that the structure designed for 475 years return period had lower resistance to fire with significant deformed state under earthquake, in comparison with the structure designed for 2475 years return period which had higher resistance to fire with insignificant deformation under earthquake.

Many researchers have focused on studying individual structural components to observe behavior when subjected to a fire. Memari *et al*. (2014) studied the impact of fire following the earthquake on the performance of a moment resistant frame with no protection and with reduced beam section connections. To determine the seismic response, nonlinear dynamic analysis was performed and to evaluate the impacts of subsequent parametric fire together with cooling phase the uncoupled thermal-mechanical analysis was performed. It was seen that when only the symmetric fire configuration was taken into account, the global performance of studied frames under post-earthquake fire

*Corresponding author, Associate Professor
E-mail: a-karam@um.ac.ir
[a]Ph.D.
E-mail: rasul.kaffash@mail.um.ac.ir

ISSN: 2092-7614 (Print), 2092-7622 (Online)

was not affected by the earthquake.

Behavior of tall steel structures under vertically travelling fires have been studied by Behnam and Ronagh (2014). Behnam (2016) has also made a comparison between the post-earthquake fire performances of regular and irregular tall steel structures. The results of this study showed that the irregular steel structures had been more damaged with respect to the regular ones and consequently had lower resistance to fire after the earthquake. Rackauskaite *et al*. 2017 have compared computationally the structural response of a multi-storey steel frame subjected to both uniform and travelling fires.

Some researchers have conducted case studies of the effect of post-earthquake fire on steel and composite structures. Pantousa and Mistakidis (2016) have developed a number of numerical models to assess the behavior of steel structures under the fire which follows after an earthquake. It was understood that the fire resistance of the structure is determined using rotational limits based on the ductility of structural members that are subjected to fire. Furthermore, Jelinek *et al*. (2017) assessed the seismic performance of steel moment resistant frames under fire following the earthquake which were designed according to Eurocode and analyzed by nonlinear dynamic method. Their study results showed that the nonlinear geometries do not have considerable effects on the behavior of the building under fire when the building is designed according to the service damage limit states cited in Eurocode. Suwondo *et al*. (2018) implemented 3d numerical models to study the impact of seismic induced damages on resistance against fire in the composite steel-frame office buildings. They demonstrated that earthquake damage could considerably lower the fire resistance in this type of buildings with delamination of fire protection as the main consequence.

This paper attempts to investigate the performance of tall steel concentrically braced frames under fire scenarios following the earthquake. For this purpose nonlinear dynamic time history analyses was implemented to simulate ground motions, also thermal-mechanical analyses were performed to simulate the prost-earthquake fires. The frame under focus was unprotected and fire was applied to the elements exposed to fire and it was assumed that the structure lacked fireproof elements or they had been spalled during the earthquake. The sample building in this study has been implemented in several studies for assessing seismic response and progressive collapse in them (Ghosh 2006). Thus evaluating their response to post-earthquake fire would provide us with good knowledge on modern performance-based design methods concerning steel structures under fire loading after an earthquake occurrence.

2. Numerical simulation

For simulation of the post-earthquake fire scenarios, there is need for multi-stage and sequential analyses. In the present study the analysis has been performed in the following steps (Behnam and Ronagh 2013), using the finite element method in ABAQUS software (Simulia Corp 2014). At the first step the static linear analysis was performed, where the structure was subjected to gravity loads. At the second step nonlinear time history analysis is performed under strong earthquake records and at the third step nonlinear implicit dynamic analysis was performed where the effects of temperature rise on the structural members subjected to fire are taken into account. In ASCE 7-10 (2010) the simultaneous combinations of gravity loads and fire loading are presented as given in Eq. (1). In the present study, the gravity load combination for an earthquake is considered because the earthquake occurs sooner than the fire.

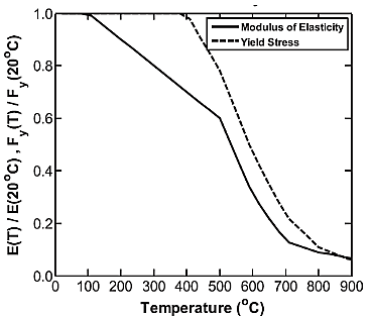

(a) Variation of modulus of elasticity and strength

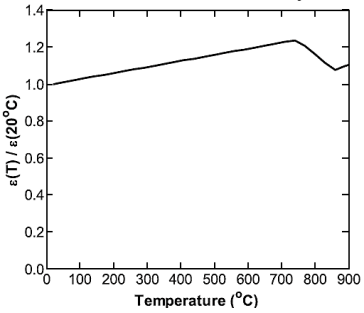

(b) Variation of thermal expansion (EN 1993-1-2 2005)

Fig. 1 Temperature-dependent mechanical, thermal, and deformational properties of structural steel (EN 1993-1-2 2005)

$$w = DL + 0.25LL \quad (1)$$

For modelling the material behavior of steel, use was made of an elastic-perfectly plastic material model. Variations of strength, stiffness and other properties of steel with temperature change were modeled according to Eurocode (2005), as demonstrated in Fig. 1. Also use has been made of the relevant steel engineering properties for the stress-strain behavior of steel in the analyses (Arasaratnam *et al*. 2011).

2.1. Earthquake load

FEMA P695 (2009) is implemented for performing nonlinear time history analysis to simulate the impact of earthquake on the structure. This guideline is consulted to select the set of ground motion records to be implemented for assessing the behavior of building using the nonlinear dynamic analysis methods. Also, the scaling methods is implemented based on this methodology. As shown in Fig. 2 and according to Table 1, five records are used for the

Table1 Near- and far-field set of records used in the present study (FEMA P695 2009)

Record number	Earthquake name	year	Mw	Recording Station	Distance (km)	PGAmax (g)	Normalization Factor	Scaling Factors
953	Northridge	1994	6.7	Beverly Hills - Mulhol	13.3	0.52	1.09	0.82
960	Northridge	1994	6.7	Canyon Country-WLC	11.9	0.48	0.65	0.82
1602	Duzce, Turkey	1999	7.1	Bolu	12.2	0.82	0.83	0.82
1111	Kobe, Japan	1995	6.9	El Centro Array #11	16.15	0.51	1.03	0.82
752	Loma Prieta	1989	6.9	Capitola	22.1	0.53	0.63	0.82

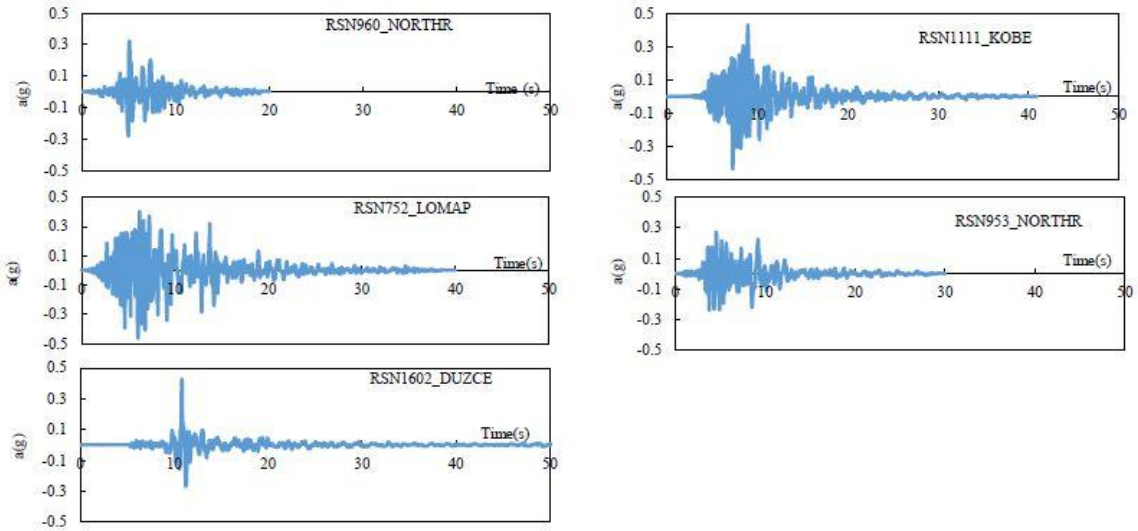

Fig. 2 All applied acceleration time histories in earthquake response analysis

analyses. Each record is named by RSN (Record Sequence Number) followed by a number as presented in Table 1. Each record contains two horizontal components and one vertical component of which only the horizontal ones are used in the analysis. As recommended in FEMA p695, individual earthquake records should be normalized with respect to peak ground velocity (PGV) to decrease dispersion of the results. On the other hand, each set of records is collectively scaled to match the median spectral acceleration of the set to the maximum considered earthquake (MCE) response spectrum corresponding to design category of 5% damping in the code-defined period of the structure. Here in this study, we have subjected the structure to fire after disappearance of earthquake dynamic effects. For this purpose each acceleration time-history is delayed by additional 20 seconds with zero acceleration to account for frame stabilization, and the fire loading analysis is performed on the stable structure with residual deformations resulted from the earthquake (Jelinek *et al*. 2017).

2.1. Fire load

Various temperature-time diagrams are available such as ISO 834-1, ASTM-E119, and eurocode parametric fire, which are used for numerical simulation of fire load. In this study the eurocode parametric fire diagram, given in Fig.3, is utilized which implements the cooling phase and yields the temperature-time diagram function of the fire load density, openings and thermal characteristics of borders of fire compartment (EN 1991-1-2 2002).

The temperature $\theta(°C)$ in the heating phase of eurocode parametric fire diagram is a function of fictitious time t* (Eq (2)) where t^* is obtained from the product $\Gamma \cdot t$. Where Γ is a dimensionless parameter which is calculated by $(O/b)^2/(0.04/1160)^2$. In this relation, O denotes an opening factor, b is the thermal absorptivity of surfaces which surround the compartment and t is the time in hours (EN 1991-1-2 2002). In this study we have taken Γ equal to unity so that a heating phase is obtained which is near to that given in the ISO 834-1 standard fire diagram (Memari *et al*. 2014). The heating phase which is approximated by ISO 834-1 fire diagram could be used for the individual members as well as the frames without any limitations, as other researchers also have applied them in their studies.

$$\theta = 20 + 1325(1 - 0.324e^{-0.2t^*} - 0.204^{-1.7t^*} - 0.472^{-19t^*}) \quad (2)$$

This formulation could be applied for a wide range of design values such as the fire load density ($q_{t,d}$), opening factor (O) and thermal absorptivity of surrounding surfaces of the compartment (b). The above parameters could be applied for both the open-plan and closed-plan office buildings. As is seen in Fig. 3, Eq. (3) yields a maximum temperature equal to of 800 °C in 22 min for a combination fire parameters of open- plan and closed-plan office building.

$$t^*_{max} = t_{max} = \max\left\{0.2 \times 10^{-3} \frac{q_{t,d}}{O}, \quad t_{lim}\right\} \quad (3)$$

If one takes t_{lim} equal to 20 min for the medium fire growth, the fire diagram would be a ventilation controlled fire. Then the cooling phase is calculated using Eq. (4),

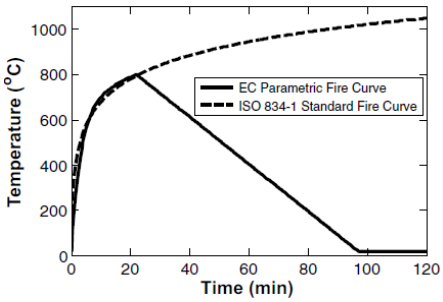

Fig. 3 Eurocode parametric fire diagram

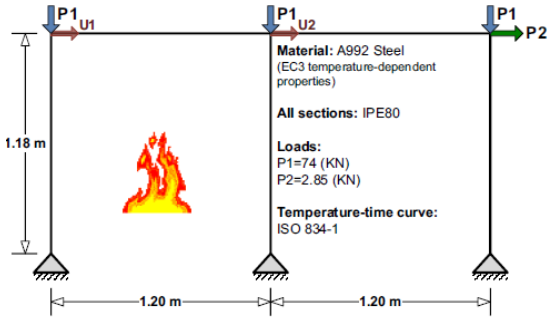

Fig. 4 The small scale steel frame used in the validation of thermal-mechanical analysis (Rubert and Schaumann September 1985)

which ends before the ambient temperature phase.

$$\theta = \theta_{max} - 625(t^* - t^*_{max}) \quad (4)$$

Ultimately the ambient temperature after fire is extinguished is assumed to terminate at 120 min (Memari *et al*. 2014). In reinforced concrete buildings this assumption that the temperature generated by the source of fire and the temperature at the surface of structural components is equal, would not be correct. But in steel structures due to the high conductivity of steel and rapid transmission of heat, this assumption is correct. It is assumed that for exposed structural components the temperature distribution across the section is uniform (EN 1993-1-2 2005).

2.3. Post-earthquake fire scenarios

There is difference between travelling fire and uniform fire in terms of different structural responses which are important for structural design and choosing the critical members (Rackauskaite *et al*. 2017). Different scenarios are implemented in this study as it is not possible to determine where the fire occurs. Studies performed by Ryder *et al*. (2002) and Wang and Li (2009) demonstrated that a steel member with partial damage to fire protection is much less resistant to fire compared to a fully protected one. The post-earthquake fire could reach all members of a structure. This is due to this conservative assumption that all the fire proofing materials are damaged in the earthquake event. Here we applied fire only on the unprotected columns, braces and at the upper beams of the story exposed to fire, as the thermal conductivity of the concrete floor slab prevents heat transfer to the lower beams. Furthermore, we have assumed no collaboration between the steel beam and

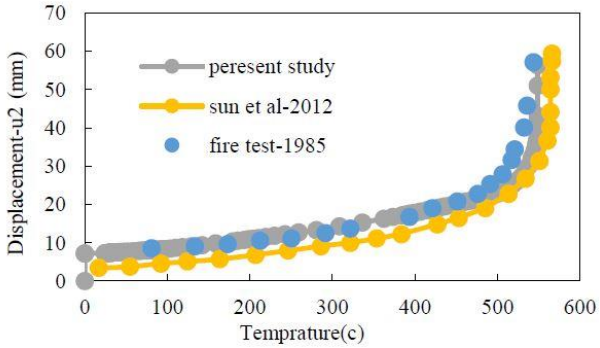

Fig. 5 Validation results of the thermal-mechanical analysis

concrete slab during the structural analysis. According to Quiel and Garlock (2008) who have recommended not considering slabs in 2D analysis of frames, the mechanical effects of concrete slabs are ignored in the thermal-mechanical analysis. Assuming full composite action between the concrete slabs and steel girders, the rapid thermal expansion created in steel girders causes large tensile forces in concrete slabs and consequently formation of cracks in them. Therefore concrete slabs carry minimum stresses and one could neglect structural effects in them due to the fire (Quiel and Garlock 2008).

2.4. Verification of the numerical models

For validation purposes a small scale steel frame which was tested at high temperature by Rubert and Schauman (1985) and then analysed by Sun *et al*. (2012) was selected (Fig.4). All structural components are of European type IPE80-I sections. The left span structural components are uniformly heated according to ISO 834-1 standard fire diagram. The model used for validation had EC3 temperature-dependent material properties (EN 1993-1-2 2005). The lateral displacements against temperature are compared at two rigid joints to the experimental and numerical studies results performed by other researchers. As seen in Fig.5 there was a good agreement with the previous studies (both numerical and experimental). So it could be stated that the proposed approach in this study is appropriate for simulation of performance of structural steel frames under fire.

For verification of the modeled structures subjected to earthquake loading, the results of large-scale shake table tests performed on the specimen used by Okazaki *et al*. (2013) are implemented. The properties of the specimen made in the laboratory and its response under earthquake records are given in Fig. 6. The specimen model is comprised of panel zones that are modeled according to Gupta and Krawinkler (1999) and a rigid segment near the connection plates (Harris and Speicher 2015). To model the test bed system the end of each beam was connected to a leaning column that supported half of the test-bed mass. In Fig. 4 the story shear against the story drift response is depicted for 70% motion, also it is shown that the experimental response was almost similar for both motions. Therefore, modeling using the nonlinear beam elements provides accurate nonlinear response of the system.

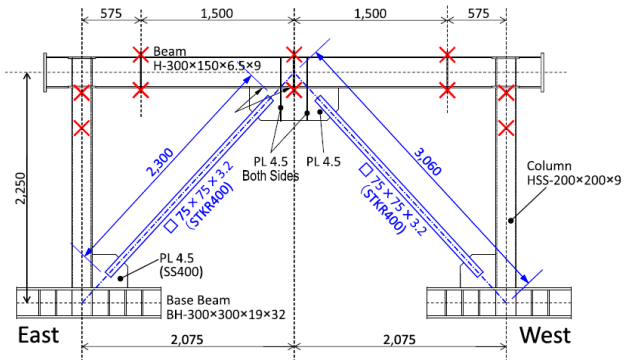

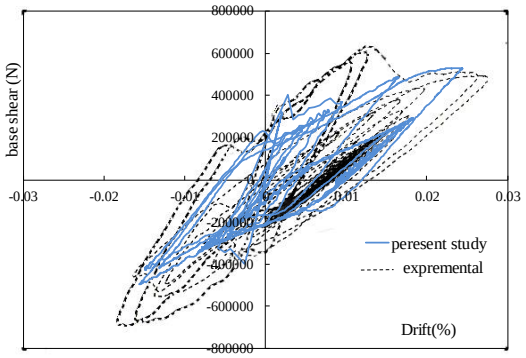

Fig. 6 Experimentally prototype steel braced frame (Okazaki *et al*. 2013) and its response by numerical simulation

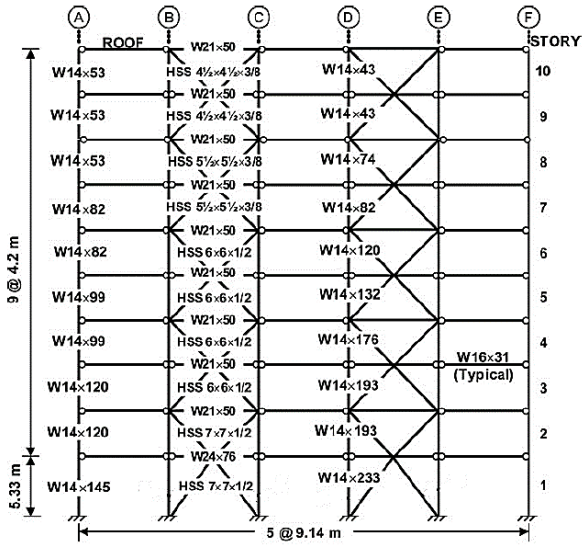

Fig. 7 Elevation of braced frame systems E–W Elevation (Line 6) (Ghosh 2006)

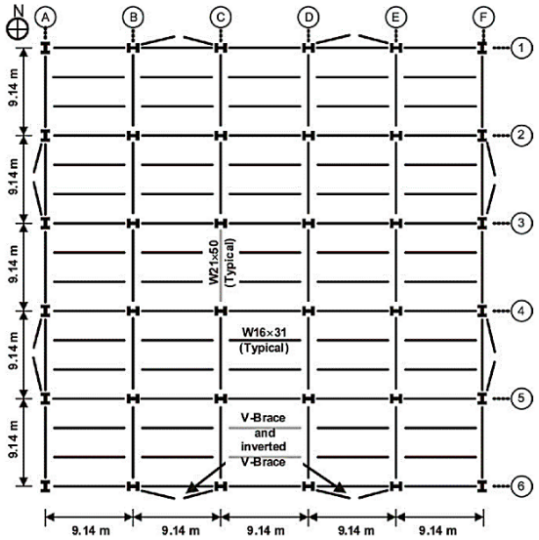

Fig. 8 Plan layout for braced frame systems (Ghosh 2006)

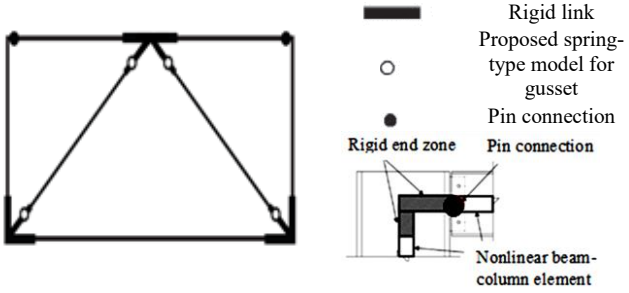

Fig. 9 Schematic model of SCBF panel (Hsiao *et al*. 2012)

3. Numerical analysis

In the present study one case of steel braced frame structure designed in NIST (Ghosh 2006) was chosen to assess the performance of tall braced frames under fire loading. The designed prototype was used to assess its response to fire loading after earthquake which may result in progressive collapse. The building is a 10-story office with dimensions of 45.7 m × 45.7 m in plan which uses braced frames as the lateral load resisting system. The building is designed to resist moderate earthquakes and utilizes SCBFs according to AISC seismic provisions (2005). Fig. 7 depicts the East-West frames chosen to study. Also, the plan views of the building are shown in Fig. 8. ASCE 7-05 (2005) is used for determining the design loads. The materials and design standards given in references (AISC 341-05 2005; AISC 360-05 2005; AISC 2006; IBC 2006), are used for design of the structural components and their connections.

The assumed dead loads for typical floors are comprised of the slab self-weight which is 2200 N/m2, and superimposed load which is 1430 N/m2, and the design live load which is taken equal to 4790 N/m2. Also concerning the roof, the slab self-weight is taken equal to 2200 N/m2, the superimposed dead load and design live load are taken equal to 480 N/m2 and 960 N/m2, respectively. The structural building system that is adopted is comprised of braced frames and the gravity system. The columns and beams are connected by shear type connections in the gravity system. The braces are square, seismically compact with hollow steel sections (HSS). The braces are selected from ASTM A500 grade B steel (Fy=317 MPa), whereas all the beams and columns are of A992 structural steel (Fy=345 MPa) type. As seen in Fig. 10 the buildings are simplified using the two dimensional frame models, also frame elements are modelled using the 2-node Bernoulli beams. The maximum length used for the finite elements is 1 m, whereas the finest mesh with 0.35 m is used around the joints for accurate simulation of plastic hinges formed in the

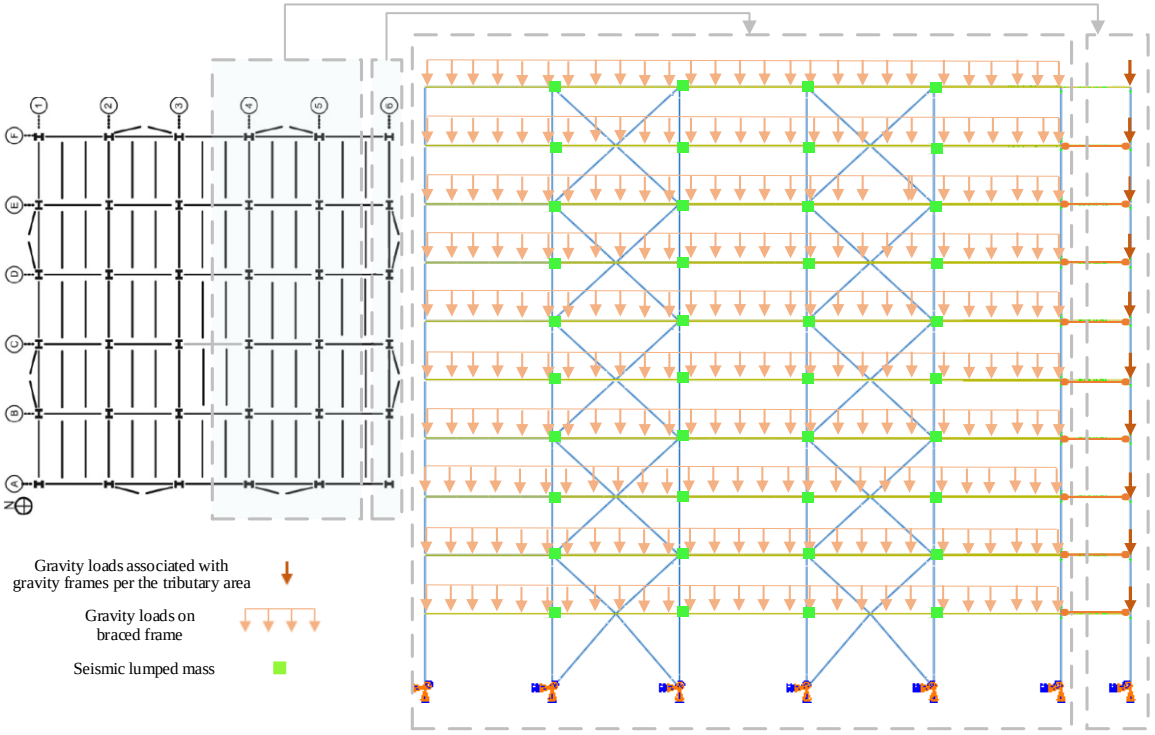

Fig. 10 Finite element model of the steel braced frame for illustration

vicinity of beam-column joints. A small initial camber was applied at the middle of brace to cause buckling. Uriz (2005) study recommends applying the initial camber at 0.05% and 0.1% distances of brace length. For simulation of the out-of-plane rotational behavior of connections in gusset plates, use was made of single springs along the brace axial direction and at beyond of the brace (Hsiao *et al.* 2012). The initial stiffness of the rotational spring was determined according to the gusset plate properties and its geometry. As shown in Fig. 9, use was made of rigid links to simulate the remainder of gusset plate. The beam-column connections where there is no gusset plate were of shear-plate type connections. The beam-column-brace connections were of welded flange welded web connection type as they acted as fully restrained with fixed connections.

For simplification purpose all other beam-column connections were selected of simply pinned type. The columns were taken as fixed at their base so that could resist lateral forces with strong-axis in the bending direction. Also the beams were laterally supported at the quarter points along the span length. To account for the stiffening effect of gusset plate and the physical size, rigid offsets were assumed at the beam-column and brace-to-framing connections. The effective length of the braces was taken equal to 70% of the work-point-to-work-point length. No failure is assumed at the connections in the modelling.

The gravity loads are divided into two types of gravity and concentrated loads. The gravity loads corresponding to braced frame are applied as distributed vertical forces over the beams length at the level of each story. The concentrated loads are associated with interior gravity frames per tributary area and are applied to the leaning columns at the related story levels (Fig. 10).

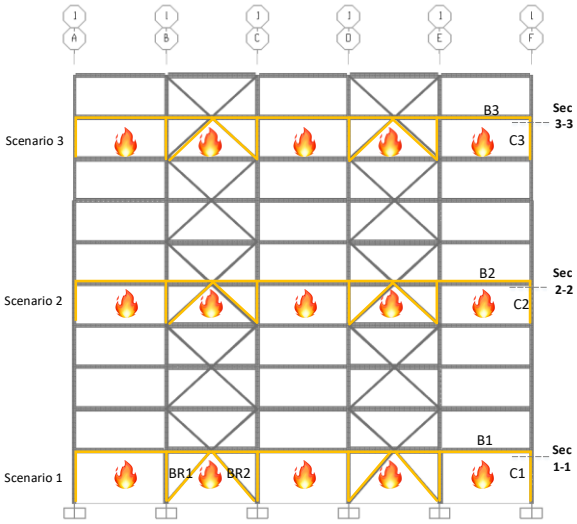

Fig. 11 Fire scenarios

We need to representation of gravity frames by leaning columns to account for the P-Δ effects. For this purpose a co-rotational method is utilized. As seen in Fig. 10, the leaning column is modeled by truss elements. For the connection to the main frame at each floor level the multi-point constraint (MPC) links are implemented. The leaning column is pinned at the base and floor levels and is axially stiff so it would have no impact on the lateral stiffness of the main frame.

Three scenarios are considered in this study which are fire occurrence on; (a) ground-floor, (b) fourth floor and (c) eighth floor (Fig. 11). In all the above-mentioned scenarios

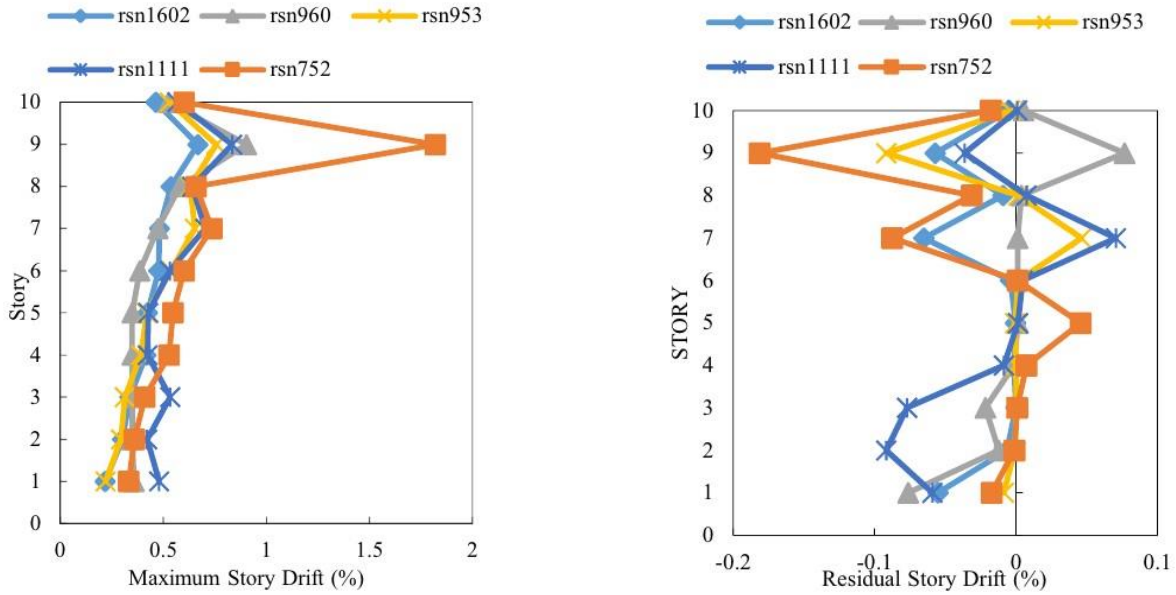

Fig. 12 Braced frame response under selected records

fire loading was applied to the columns, braces and upper beams of the floor which is under fire. Also, the floor subjected to the fire loading is taken as the fire compartment.

3.1. Analysis results

The structural performance of braced frame under earthquake is assessed by implementing ASCE 41-06 (2007). Also other post-earthquake seismic evaluation method was proposed that uses displacement and acceleration measurements taken from real structural responses that resulted during an earthquake (Hsu and pham 2019). The structural performance is dependent upon the inter-story drift ratio (IDR) and residual drift.

As stated in ASCE 41-06, the structural performance levels for steel braced frames are comprised of immediate Occupancy (IO), Life Safety (LS), and Collapse Prevention (CP) where the IDR value is smaller than 0.5%, 1.5% and 2.0%, respectively. Also, the residual drift value is smaller than 0, 0.5%, and 2 %, respectively. As seen in Fig. 12, the structural performance level of the steel braced frame under introduced records corresponds to the Collapse Prevention (CP) level.

Fig. 13 illustrates the post-earthquake fire (pef) resistance of the structure in scenario 1 and when exposed to direct fire (df) without earthquake with uniform distribution of fire over the ground floor. The fire resistance is defined as a time duration at which the displacements, either globally or locally, go beyond the chosen thresholds. The thresholds were identified by the curve for displacements versus time step merging towards the vertical asymptote (Almand, Phan *et al*. 2004). For the comparison purposes a simultaneous df event also has been shown in Fig. 13.

As depicted in Fig. 13, according to scenario 1 the df resistance of braced frame is about 12 minutes and 12 seconds and for pef resistance this value is on average about 11 minutes and 36 seconds. It is observed that for the ground floor fire the df resistance is somehow higher than that of pef. Fig. 14 depicts the lateral displacement against time for scenario 2. Here the df resistance is 13 minutes and 6 seconds which is slightly lower than the previous scenario. Also, the pef resistance of the braced frame for this scenario is on average about 13 minutes and 24 seconds. Fig. 15 depicts both the pef and df resistances for scenario 3. The df fire at eighth floor, similar to the previous scenarios, resulted in collapse in about 19 minutes and 42 seconds, but its pef resistance was on average about 18 minutes and 48 seconds.

Generally, comparing the duration of structure resistance under fire loading and fire after earthquake loading, (neglecting some exceptions) it is found that regardless of the records properties, the braced frame resistance to fire is not influenced by the earthquake. Also, it is found that the earthquake had slightly decreased the fire resistance duration in scenarios 1 and 3. Through examining the structure residual deformations under different seismic records it is found that the plastic deformations at the lower bracing elements and at their top had been the cause of this issue.

To study the braces behavior, the corresponding history of the internal axial forces generated in some heated braces in scenario 1, which are subjected to both the df and pef loadings, are derived and given in Figs. 16-19. Furthermore, the tensile capacity and buckling load of the braces which are calculated using AISC 340-05 (2005) are shown in the corresponding diagrams.

As seen, in the case of df loading, by increase in the temperature and axial expansion of the braces, they lost their resistance and then their compressive axial force was reduced. On the other hand increased heating and development of asymmetric deformation in the structure together with P-Δ effect, leads to increased relative lateral

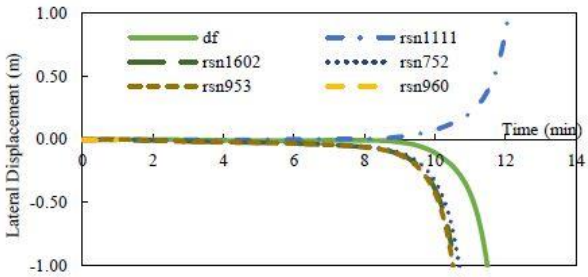

Loading type	Record number	Resistance time
pef	rsn1111	13 minutes and 6 seconds
	rsn1602	11 minutes and 18 seconds
	rsn752	11 minutes and 24 seconds
	rsn953	11 minutes and 12 seconds
	rsn960	11 minutes and 12 seconds
df	---	12 minutes and 12 seconds

Fig. 13 Fire resistance for pef and df loading based on scenario 1

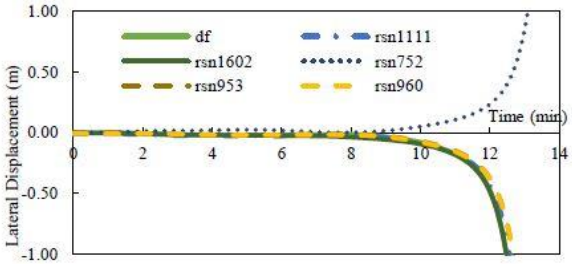

Loading type	Record number	Resistance time
pef	rsn1111	13 minutes and 12 seconds
	rsn1602	13 minutes and 6 seconds
	rsn752	13 minutes and 54 seconds
	rsn953	13 minutes and 18 seconds
	rsn960	13 minutes and 18 seconds
df		13 minutes and 6 seconds

Fig. 14 Fire resistance for pef and df loading based on scenario 2

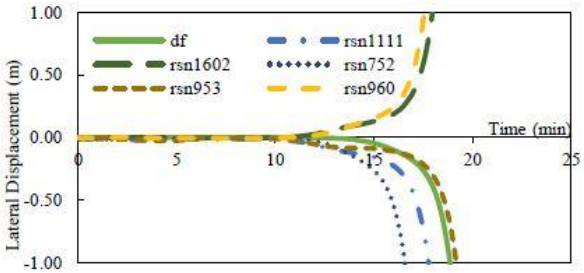

Loading type	Record number	Resistance time
pef	rsn1111	18 minutes and 42 seconds
	rsn1602	19 minutes and 6 seconds
	rsn752	17 minutes and 30 seconds
	rsn953	20 minutes and 6 seconds
	rsn960	18 minutes and 42 seconds
df		19 minutes and 42 seconds

Fig. 15 Fire resistance for pef and df loading based on scenario 3

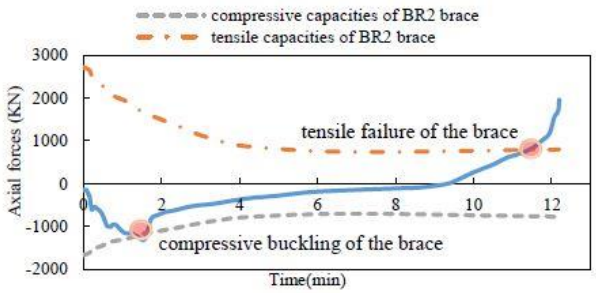

Fig. 16 Axial force time history in the BR2 brace in case of DF based on scenario 1

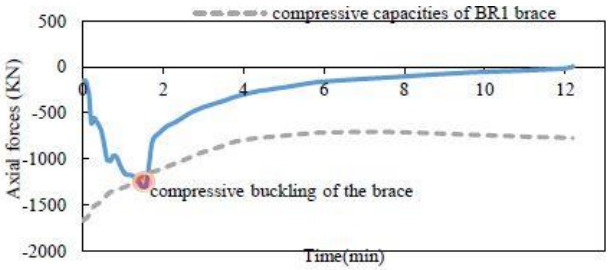

Fig. 17 Axial force time history in the BR1 brace in case of DF based on scenario 1

displacement of the floor and subsequent generation of tensile forces in a number of pre-buckled braces. Increased tensile forces in the braces and exceeding the ultimate tensile capacity in them results in the braces failure. This event combined with loss of resistance of the columns under fire causes total collapse of the floor.

Also, investigating the internal forces generated in the braces after a post-earthquake fire, one could observe that due to the earthquake the internal forces in some braces exceed their tensile or compressive capacities leading to their deformation. This causes reduction in their residual load capacity and these effects lower their resistance to fire.

Comparing Figs. 16-19 which depict the fire resistance of members subjected to fire and Figs. 13-15 which depict the overall resistance of the structure against fire one could conclude that the duration of fire resistance of the structure is in proportion with the tensile failure duration of the heated braces at the end of fire phase.

Among the main findings concerning the steel braced frame elements behavior subjected to fire one could refer to the internal forces generated due to the heated beams which exceed the yield threshold at high temperatures. This in turn occurs due to the large compressive axial forces developed as the result of lateral constraints on the expansion of beams. Large axial forces are generated in the beams when

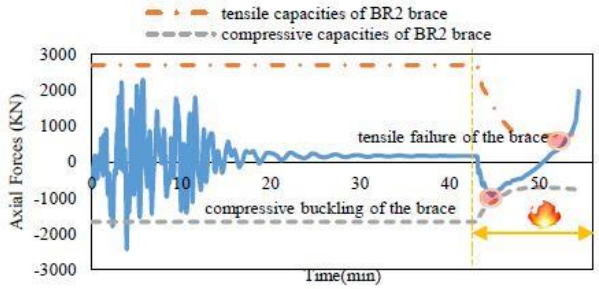

Fig. 18 Axial force time history in the BR2 brace in case of PEF under rsn752 record and scenario 1

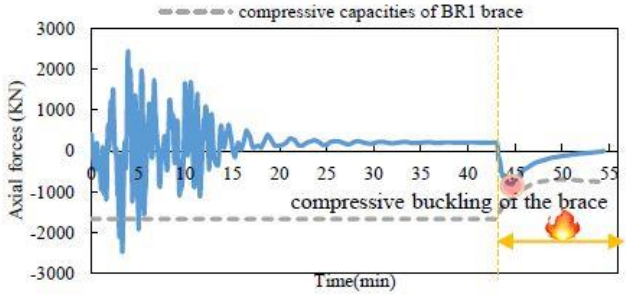

Fig. 19 Axial force time history in the BR1 brace in case of PEF under rsn752 record and scenario 1

they are subjected to the heating phase and the axial expansion caused considerable moments in columns at both beam ends. Thus examining the interaction between axial force and bending moment in beams and columns is essential in assessing their performance during a post-earthquake fire. Eq. (5) which represents the axial force-bending moment interaction (AISC 360-10 2010) is applied for the chosen braced frame beams and columns.

$$\frac{P_r(T)}{2P_n(T)}+\frac{M_r(T)}{M_n(T)}\le 1 \ \ for \ \ \frac{P_r(T)}{P_n(T)}<0.2$$
$$\frac{P_r(T)}{P_n(T)}+\frac{8}{9}\frac{M_r(T)}{M_n(T)}\le 1 \quad \text{for} \quad \frac{P_r(T)}{P_n(T)}\ge 0.2 \tag{5}$$

In the above equation Pn(T) denotes the nominal compressive or tensile strength which is a function of temperature and Mn(T) represents the nominal flexural strength. Details concerning the calculation of Pn(T) and Mn(T) are given in AISC Specification (2010). In addition Pr (T) and Mr (T) are respectively the required axial compressive or tensile force and bending moment of the structural components which are functions of the temperature. Fig. 20 depicts the internal forces generated in a beam subjected to fire for one fire scenario. Also when axial force history of the selected structural components is placed in the bending-axial interaction relation, one could present the bending capacity as a function of time. The history of axial force in the beam subjected to heat reveals that in the heated phase, the increase in compressive axial force causes that the internal forces reach the yield interaction threshold. The interaction ratio using Eq. (5) for beams B1 (Fig. 11) at a temperature equal to 130 °C, reaches the yield interaction threshold. Also, as the modulus of elasticity is considerably reduced, the compressive axial

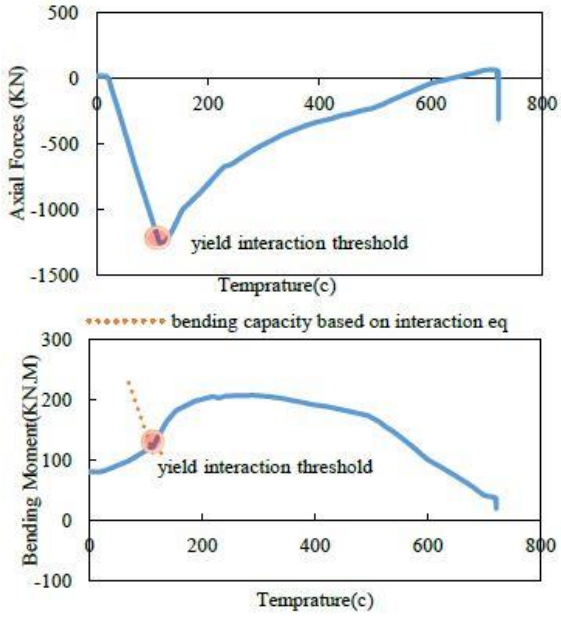

Fig. 20 Internal forces history in mid-span of B1 beam based on scenario 1

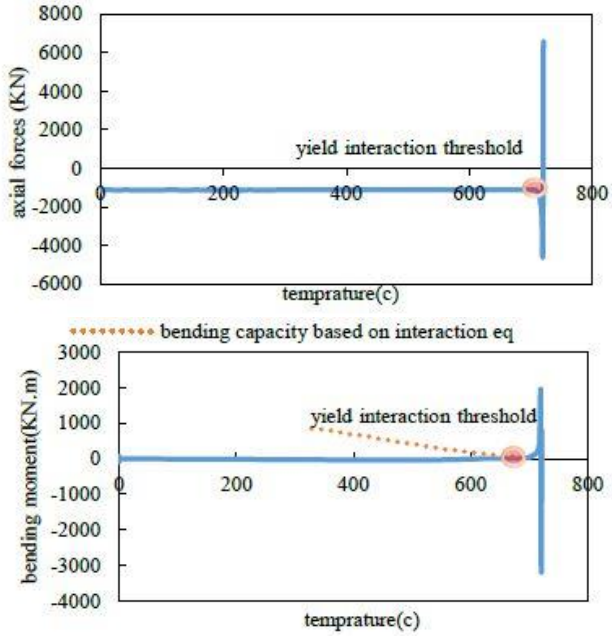

Fig. 21 Internal forces history in sec 1-1 of C1 critical column during scenario 1

force was decreased which reached almost the zero axial compressive force near 600 °C. this reduction of the compressive axial forces in beams is specially intensified at 500 °C, that is where the modulus of elasticity drops suddenly.

Fig. 21 shows the internal forces generated in a heated corner column for the one fire scenarios. Here also one could place the axial force history of the selected structural components in the bending-axial interaction equation to obtain the amount of bending capacity of that component at the yield interaction threshold which is a function of the temperature.

As seen, the bending moment in the column subjected to heating is the result of catenary action of the exposed beams on the column. Also it could be seen that by increase of the bending moment in column, the interaction ratio calculated by Eq. (5) for column C1 reaches the yield interaction threshold at temperatures near 680 ° C. The column finally collapses due to the P-Δ effect and lateral displacement.

4. Summary and conclusions

In this study the performance of a tall steel concentrically braced frame subjected to the fire following an earthquake is assessed under five different earthquake records and three different fire scenarios using the recent methods implemented for earthquake and subsequent fire loadings. Furthermore, three fire loading scenarios were used without a prior earthquake. The conclusions derived from the analyses are as follows:

Comparison of the post-earthquake fire resistance analysis subjected to different records shows that there is not considerable difference between the results of the examined records. The post-earthquake fire scenarios on the ground, fourth and eight stories yielded 11.6, 13.4 and 18.8 minutes fire durations, respectively. Whereas these fire scenarios without a prior earthquake and for the above mentioned floors yielded 12.2, 13.1 and 19.7 minutes fire durations, respectively.

Investigating the axial force in the beams subjected to earthquake and subsequent fire loading revealed that the axial compressive force at the start of heated phase increased first due to expansion of the beams, so that the ratio of bending-axial interaction at 130 °C reached the yield threshold value and then the axial compressive force decreased due to considerable decrease in the modulus of elasticity.

Examining different post-earthquake fire scenarios shows that the catenary action in the beams and the axial force generated at the joints leads to yield threshold of the columns during high temperatures.

Investigating the internal forces developed in the braces for a post-earthquake fire revealed that the internal forces in them have exceeded the tensile and compressive capacities as the result of earthquake. Also deformation of the braces has caused reduction in the residual load capacity and subsequent reduction in the fire resistance. Furthermore, comparing between resistance of the braces subjected to high temperature and overall fire resistance of the structure shows that the fire resistance duration of the structure is in proportion to the tensile failure of the heated braces at the end of fire heating phase.

Studying the resistance duration of the structures subjected to post-earthquake fire loading and that of fire only loading per different fire scenarios, revealed that this duration at lower story levels was much less than the higher level stories, and at lower levels due to increased gravity loads the effect of P-Δ is increased. Consequently, the post-earthquake fire scenario at lower level stories increases the potential of early structural damage.

As fire may occur alternatively at different classes, so it is essential to investigate the results of delayed fires to reach more realistic results.

References

EN 1991-1-2 (2002), *Eurocode1: Action on Structures – Part 1-2: General Actions – Actions on Structures Exposed to Fire*, European Committee for Normalization, Brussels, Belgium.

ANSI/AISC 341-05 (2005), *Seismic Provisions for Structural Steel Buildings*, American Institute of Steel Construction, Chicago, U.S.A.

ANSI/AISC 360-05 (2005), *Specifications for Structural Steel Buildings*, American Institute of Steel Construction, Chicago, U.S.A

ASCE 7-05 (2005), *Minimum design Loads for Buildings and Other Structures*, American Society of Civil Engineers, Virginia, U.S.A.

EN 1993-1-2 (2005), Eurocode3: Design of Steel Structures, Part1–2: GeneralRules- Structural Fire Design, European Committee for Normalization, Brussels, Belgium.

AISC Steel Construction Manual (2006), American Institute of Steel Construction, Chicago, U.S.A.

International Building Code (IBC) (2006), International Code Council.

ASCE/SEI 41-06 (2007), *Seismic Rehabilitation of Existing Buildings*, ASCE Reston, VA,

FEMA P695 (2009), *Quantification of Building Seismic Performance Factors*, Federal Emergency Management Agency, Washington, U.S.A.

ANSI/AISC 360-10 (2010), *Specifications for Structural Steel Buildings*, American Institute of Steel Construction, Chicago, U.S.A.

ASCE 7-10 (2010), *Minimum Design Loads for Buildings and Other Structures*, American Society of Civil Engineers, Virginia, U.S.A.

Almand, K., Phan, L., McAllister, T., Starnes, M. and Gross, J. (2004), *NET-SFPE Workshop for Development of a National R&D Roadmap for Structural Fire Safety Design and Retrofit of Structures*, National Institute of Standards and Technology.

Arasaratnam, P., Sivakumaran, K.S. and Tait, M.J. (2011), *True Stress-True Strain Models for Structural Steel Elements*, International Scholarly Research Notices.

Behnam, B. (2016), *Post-Earthquake Fire Analysis in Urban Structures*, CRC Press, Boca Raton.

Behnam, B. (2016), "Structural response of vertically irregular tall moment-resisting steel frames under pre- and post-earthquake fire", *Struct. Des. Tall Spec. Build*.. **25**(12), 543-557. https://doi.org/10.1002/tal.1271.

Behnam, B. and Ronagh, H.R. (2013), "Post-earthquake fire performance-based behavior of reinforced concrete structures", *Earthq. Struct*., **5**(4) 379-394. https://doi.org/10.12989/eas.2013.5.4.379.

Behnam, B. and Ronagh, H.R. (2014), "Behavior of moment-resisting tall steel structures exposed to a vertically traveling post-earthquake fire", *Struct. Des. Tall Spec. Build*., **23**(14), 1083-1096. https://doi.org/10.1002/tal.1109.

Dassault Systèmes Simulia Corp (2014), *ABAQUS 6.14 Documentation*, Dassault Systèmes Simulia Corp, RI, U.S.A.

Della Corte, G., Faggiano, B. and Mazzolani, F. (2005), "On the structural effects of fire following an earthquake", *Improvement of Building's Structural Quality by new Technologies-COST C12 Final Conference Proceedings*, Taylor and Francis, London.

Faggiano, B., De Gregorio, D. and Mazzolani, F. (2010), "Assessment of the robustness of structures subjected to fire following earthquake through a performance-based approach", *Proc. Int. Conference Urban habitat constructions under*

catastrophic events (COST C26 Action), Naples, Italy.
Faggiano, B., Esposto, M. and Mazzolani, F. (2007), "Fire analysis on steel portal frames damaged after earthquake according to performance based design", *Proceedings Workshop Urban Habitat Construction under Catastrophic Events*, Czech Republic.
Ghosh, S.K. (2006), *Assessing Ability of Seismic Structural Systems to Withstand Progressive Collapse: Design of Steel Braced Frame Buildings*, The National Institute of Standards and Technology.
Gupta, A. and Krawinkler, H. (1999), *Seismic Demands for Performance Evaluation of Steel Moment Resisting Frame Structures*, Dept. of Civil and Environmental Engineering Stanford Univ.
Harris, J. and Speicher, M. (2015), *Assessment of First Generation Performance-Based Seismic Design Methods for New Steel Buildings, Volume 3: Eccentrically Braced Frames*, Technical Note (NIST TN), National Institute of Standards and Technology, Gaithersburg. https://doi.org/10.6028/NIST.TN.1863-3
Hsu, T.Y. and Pham, Q.V. (2019), "Post-earthquake assessment of buildings using displacement and acceleration response", *Earthq. Struct*., **17**(6), 599-609. https://doi.org/10.12989/eas.2019.17.6.599.
Hsiao, P.C., Lehman, D.E. and Roeder, C.W. (2012), "Improved analytical model for special concentrically braced frames", *J. Construct. Steel Res*., **73**, 80-94, https://doi.org/10.1016/j.jcsr.2012.01.010.
Jelinek, T., Zania, V. and Giuliani, L. (2017), "Post-earthquake fire resistance of steel buildings", *J. Construct. Steel Res*., 138, 774-782.
Memari, M., Mahmoud, H. and Ellingwood, B. (2014), "Post-earthquake fire performance of moment resisting frames with reduced beam section connections", *J. Construct. Steel Res*., **103**, 215-229. https://doi.org/10.1016/j.jcsr.2014.09.008.
Okazaki, T., Lignos, D.G., Hikino, T. and Kajiwara, K. (2013), "Dynamic response of a chevron concentrically braced frame", *J. Struct. Eng*., **139**(4), 515-525. https://doi.org/10.1061/(asce)st.1943-541x.0000679.
Pantousa, D. and Mistakidis, E. (2016), "Fire-after-earthquake resistance of steel structures using rotational capacity limits", *Earthq. Struct*., **10**(4), 867-891.
Quiel, S.E. and Garlock, M.E. (2008), "Modeling high-rise steel framed buildings under fire", *In Structures Congress 2008: Crossing Borders*.
Rackauskaite, E., Kotsovinos, P., Jeffers, A. and Rein, G. (2017), "Structural analysis of multi-storey steel frames exposed to travelling fires and traditional design fires", *Eng. Struct*., **150**, 271-287. https://doi.org/10.1016/j.engstruct.2017.06.055.
Rubert, A. and Schaumann, P. (1985), "Tragverhalten stählerner Rahmensysteme bei Brandbeanspruchung", *Stahlbau*. 54, 280-287
Ryder, N., Wolin, S. and Milke, J. (2002), "An investigation of the reduction in fire resistance of steel columns caused by loss of spray-applied fire protection", *J. Fire Protection Eng*., **12**(1), 31-44.
Scawthorn, C., Eidinger, J.M. and Schiff, A. (2005), *Fire Following Earthquake*, American Society of Civil Engineers (ASCE), Reston, Virginia, U.S.A.
Sun, R., Huang, Z. and Burgess, I.W. (2012), "Progressive collapse analysis of steel structures under fire conditions", *Eng. Struct*., **34**, 400-413. https://doi.org/10.1016/j.engstruct.2011.10.009.
Suwondo, R., Gillie, M., Cunningham, L. and Bailey, C. (2018), "Effect of earthquake damage on the behaviour of composite steel frames in fire", *Advan. Struct. Eng*., **21**(16), 2589-2604.
Uriz, P. (2005), *Towards Earthquake Resistant Design of Concentrically Braced Steel Structures*, University of California, Berkeley, California.
Wang, W.Y. and Li, G.Q. (2009), "Fire-resistance study of restrained steel columns with partial damage to fire protection", *Fire Safety J*., **44**(8), 1088-1094. https://doi.org/10.1016/j.firesaf.2009.08.002.
Zaharia, R. and Pintea, D. (2009), "Fire after earthquake analysis of steel moment resisting frames", *Int. J. Steel Struct*., **9**(4), 275-284. https://doi.org/10.1007/bf03249501.

DK